

# Causal Front-Door Adjustment for Robust Jailbreak Attacks on LLMs

Yao Zhou <sup>\*12</sup> Zeen Song <sup>\*12</sup> Wenwen Qiang <sup>12</sup> Fengge Wu <sup>12</sup> Shuyi Zhou <sup>23</sup> Changwen Zheng <sup>12</sup> Hui Xiong <sup>4</sup>

## Abstract

Safety alignment mechanisms in Large Language Models (LLMs) often operate as latent internal states, obscuring the model’s inherent capabilities. Building on this observation, we model the safety mechanism as an unobserved confounder from a causal perspective. Then, we propose the Causal Front-Door Adjustment Attack (CFA<sup>2</sup>) to jailbreak LLM, which is a framework that leverages Pearl’s Front-Door Criterion to sever the confounding associations for robust jailbreaking. Specifically, we employ Sparse Autoencoders (SAEs) to physically strip defense-related features, isolating the core task intent. We further reduce computationally expensive marginalization to a deterministic intervention with low inference complexity. Experiments demonstrate that CFA<sup>2</sup> achieves state-of-the-art attack success rates while offering a mechanistic interpretation of the jail-breaking process.

## 1. Introduction

Large Language Models (LLMs) (Qi et al., 2024; Chao et al., 2024b; Liu et al., 2024a) have revolutionized human-computer interaction, yet they expose significant safety vulnerabilities. Even models aligned with rigorous safety protocols can be manipulated to generate harmful content through jailbreaking attacks (Zhang & Wei, 2025; Liu et al., 2024b; Li et al., 2024b). However, while existing optimization-based attacks, e.g., GCG, PAIR (Zou et al., 2023b; Chao et al., 2024b), achieve high success rates on specific benchmarks, they exhibit a critical weakness: instability.

Empirical studies (Rando & Tramer, 2024; Zhang et al., 2024a) demonstrate that minor semantic perturbations, e.g., synonym substitution or syntactic reordering, can cause suc-

<sup>\*</sup>Equal contribution <sup>1</sup>Institute of Software Chinese Academy of Sciences, Beijing, China <sup>2</sup>University of Chinese Academy of Sciences, Beijing, China <sup>3</sup>Institute of Information Engineering Chinese Academy of Sciences, Beijing, China <sup>4</sup>Hong Kong University of Science and Technology, China, Hong Kong, China. Correspondence to: Wenwen Qiang < qiangwenwen@iscas.ac.cn>.

Preprint. February 6, 2026.

cessful attacks to collapse. We hypothesize that this fragility stems from a fundamental limitation: existing methods rely on fitting surface-level statistical correlations between adversarial prompts and outputs. By neglecting the internal mechanisms that govern model refusal, they fail to establish a robust pathway to bypass safety guardrails.

To address this instability, we investigate the underlying generation mechanism of LLMs through a causal lens. Our approach leverages the insight that safety alignment may act as a superficial constraint rather than erasing underlying knowledge (Zhou et al., 2023; Wei et al., 2023a). Specifically, pre-trained models inherently possess the capability to answer harmful queries, but this capability is suppressed by a latent safety mechanism introduced during alignment. In causal terms, jailbreak failures occur not because the model “cannot” answer, but because the safety mechanism acts as a confounder that interferes with the output.

Building on this insight, we formulate a Structural Causal Model (SCM), as illustrated in Figure 1. Let  $X$  denote the harmful query and  $Y$  the response. We introduce an unobserved node  $U$  to represent the internal safety mechanism (e.g., RLHF alignment). Crucially,  $U$  acts as a confounder: it influences how the query is processed (path  $U \rightarrow A$ ,  $A$  is the model’s internal latent representation of  $X$ ) and directly biases the output towards refusal ( $U \rightarrow Y$ ). This confounding effect explains why simple optimization fails; that is, it cannot distinguish confounded associations between the model’s true capability and the safety interference.

To eliminate this confounding effect, we leveraging Pearl’s Front-Door Adjustment (Pearl, 2009). We introduce an observable mediator  $S$ , representing the core task semantics of the query. By ensuring that the causal influence of  $X$  on  $Y$  is mediated through  $S$ , and that  $S$  is independent of the safety mechanism  $U$ , we can isolate the true causal effect of the query on the response, bypassing the unobserved safety guardrails. Finally, we propose the Causal Front-Door Adjustment Attack (CFA<sup>2</sup>), a framework that translates this causal theory into a practical, efficient attack algorithm. Specifically, CFA<sup>2</sup> implements this framework via a two-stage pipeline: First, employing Sparse Autoencoders with contrastive analysis to extract interpretable features and disentangle invariant task semantics from defense mechanisms; and second, applying weight orthogonalization to

physically the defense subspace, reducing the adjustment to a deterministic forward pass with  $O(1)$  complexity.

Our key contributions: (1) We propose a **Causal Jailbreaking Framework**, the first approach to model safety mechanisms as unobserved confounders within a Structural Causal Model (SCM). By applying the Front-Door Criterion, we theoretically demonstrate how to physically sever the confounding link to effectively recover suppressed model capabilities. (2) We introduce a training-free method, **CFA<sup>2</sup> Algorithm via Weight Orthogonalization**. We operationalize this framework using Sparse Autoencoders (SAEs) to interpretably isolate invariant “task intent” features. Crucially, we employ *Weight Orthogonalization* to physically strip defense subspaces, reducing complex causal marginalization to a deterministic forward pass with  $O(1)$  inference complexity. (3) We achieve **SOTA Performance and Stealthiness**. Extensive experiments demonstrate that CFA<sup>2</sup> attains a state-of-the-art 83.68% average Attack Success Rate (ASR). Unlike optimization-based attacks that often produce incoherent gibberish, our method preserves high stealthiness and naturalness in the prompt.

## 2. Related Works

**LLM Jailbreak.** Existing jailbreak methodologies broadly fall into three paradigms: optimization-based adversarial attacks (Zou et al., 2023b; Liu et al., 2024a; Zhang & Wei, 2025; Zhou et al., 2024; Jones et al.), semantic manipulation (Chao et al., 2024b; Li et al., 2024b; Mehrotra et al., 2024b; Chen et al., 2024; Li et al., 2024a; Shah et al., 2023; Yong et al., 2024; Deng et al., 2024; Yuan et al., 2024; Jin et al., 2024; Yao et al., 2024), and fine-tuning or decoding interventions (Zhang et al., 2024a; Huang et al., 2023). These approaches range from searching for adversarial suffixes that maximize harmful probability to leveraging in-context learning for linguistic obfuscation or directly disrupting alignment via weight updates. Despite their empirical success, recent evaluations reveal a critical vulnerability: severe instability. Studies by Pathade et al. (Pathade, 2025) and Liu et al. (Liu et al., 2024c) demonstrate that attack transferability is remarkably poor across different architectures and highly sensitive to random seeds. We argue that these limitations stem from a fundamental issue: current methods primarily exploit surface-level correlations between prompt patterns and refusal failures, rather than targeting the underlying causal mechanisms governing model behavior.

**Representation Learning and Mechanistic Interpretability.** To move beyond surface correlations and probe the internal decision-making processes of LLMs, representation learning offers a critical methodological pathway. While techniques like Representation Engineering (RepE) have successfully steered model behavior via dense activations (Zou et al., 2023a), they remain fundamentally con-

strained by *polysemanticity*, where single neurons encode multiple unrelated concepts, preventing precise disentanglement (Elhage et al., 2022). To address this, SAE utilizes high-dimensional sparse projections to resolve feature superposition, successfully isolating mono-semantic features ranging from coding logic to safety biases (Huben et al., 2023; Bricken et al., 2023; Templeton, 2024). However, current SAE research is predominantly limited to descriptive analysis or benign steering (e.g., enhancing honesty) (Subramani et al., 2022), leaving their potential for adversarial red-teaming largely unexplored.

## 3. Problem Formulation and Causal Analysis

In this section, we establish the theoretical foundation for our proposed method. We begin by formally defining the objective of jailbreak attacks and introducing the mathematical notations in Section 3.1. Building on this formulation, we then transition to a causal perspective in Section 3.2. Here, we construct a Structural Causal Model (SCM) to characterize the interference of unobserved safety mechanisms and apply the Front-Door Adjustment to theoretically derive a robust jailbreaking strategy.

### 3.1. Problem Formulation

In this subsection, we formally define the objective of the LLM jailbreak attack. Modern LLMs operate under an inherent tension: they retain vast knowledge and instruction-following capabilities from pre-training, but are constrained by safety alignment. A **jailbreak attack** is an adversarial attempt to bypass these constraints, aiming to elicit harmful, unethical, or restricted responses.

Let  $\mathcal{D} = \{x_i\}_{i=1}^N$  be a dataset of harmful requests drawn from a distribution  $P(x)$ . Given a pre-trained LLM  $\pi_\theta$ , the model defines a conditional distribution  $\pi_\theta(y | x)$  over the response space  $\mathcal{Y}$ . For any input  $x$ , the response  $y$  is sampled autoregressively, i.e.,  $y \sim \pi_\theta(\cdot | x)$ . We further define a binary judge function  $g : \mathcal{Y} \rightarrow \{0, 1\}$ , which determines whether a response  $y$  is a successful jailbreak ( $g(y) = 1$ ) or a harmless refusal ( $g(y) = 0$ ).

The objective of a jailbreak attack is to maximize the expected success rate, formally defined as:

$$P_{\text{success}} \triangleq \mathbb{E}_{x \sim P(x)} \mathbb{E}_{y \sim \pi_\theta(\cdot | x)} [\mathbb{1}[g(y) = 1]], \quad (1)$$

where  $\mathbb{1}[\cdot]$  denotes the indicator function. Intuitively, this objective aims to find the optimal strategy (e.g., input perturbations) to maximize the likelihood of harmful outputs. This essentially attempts to shift the model’s output distribution from the safe region toward the harmful space.

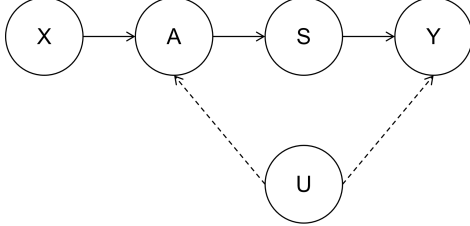


Figure 1. Jailbreaking SCM.  $X$  represents arbitrary query.  $A$  is the representation embedding of  $X$  in LLM.  $S$  denotes main semantics inherent in  $X$ .  $Y$  represents the harmful response.  $U$  represents an unobservable internal safety mechanism of the LLM.

### 3.2. Causal Analysis

From the problem formulation, our objective is to jailbreak a safety-aligned language model. In principle, a pre-trained model possesses the inherent capability to generate practical responses to arbitrary queries, regardless of their safety status. However, safety alignment introduces a constraint where the model produces refusals or templated responses for specific inputs. Crucially, such refusals do not imply a lack of underlying capability; rather, they indicate the presence of unobserved internal mechanisms (i.e., safety guardrails) that actively suppress the answer. To understand this suppression and recover the model’s answering capability, we model the interactions between queries, responses, and safety mechanisms through a causal lens.

**The Structural Causal Model (SCM).** We denote the input query by  $X$ , the response by  $Y$ , and the unobserved internal safety mechanism by  $U$ . Additionally, we introduce  $A$  to represent the model’s internal latent representation of  $X$ .

In our causal graph (see Figure 1), the path  $X \rightarrow A \rightarrow Y$  represents the model’s inherent task capability, e.g., the ideal mapping from query to representation to response in the absence of constraints. However, safety alignment introduces a confounder  $U$ . The safety mechanism  $U$  influences the internal representation  $A$  (making observed representations a mixture of task and safety signals,  $U \rightarrow A$ ) and explicitly biases the output  $Y$  towards refusal ( $U \rightarrow Y$ ) (Arditi et al., 2024; Wolf et al., 2024).

Consequently, the observed conditional distribution  $P(Y | X)$  is a mixture of the model’s potential capability and the safety mechanism’s intervention. To isolate the model’s original answering capability, we introduce an observable mediator variable  $S$ , representing the core task semantics within  $X$ . We posit that the causal effect of task information on  $Y$  is strictly mediated through  $S$ , and that  $S$  is independent of the safety mechanism  $U$ . Structurally, this decomposes the generation process into two stages: extracting the core task representation ( $X \rightarrow A \rightarrow S$ ) and generating the response conditioned on this task-specific semantic ( $S \rightarrow Y$ ). By introducing  $S$ , we isolate the mapping from  $X$  to  $Y$  driven solely by task information, effectively

filtering out the non-task safety activations present in  $A$ .

**Front-door Adjustment for Confounding Resolution.** To formally characterize the genuine influence of the input on the response while shielding the process from the safety mechanism  $U$ , we employ the causal intervention operator  $do(\cdot)$ . The objective of jailbreak is defined as the interventional distribution  $P(Y | do(A))$ . It represents the probability of generating a response in a hypothetical scenario where the structural dependency on  $U$  is logically severed.

Pearl’s Front-door Criterion (Pearl, 2009) provides the theoretical foundation for identifying  $P(Y | do(A))$  even when the confounder  $U$  is unobserved. Specifically, because the mediator  $S$  shields the direct influence of input features on  $Y$ , and the path from  $A$  to  $S$  is not intercepted by  $U$ , the causal intervention probability can be derived as:

$$P(Y = \mathbf{y} | do(A = \mathbf{a})) = \sum_s P(S = s | A = \mathbf{a}) \sum_{\mathbf{a}'} P(Y = \mathbf{y} | A = \mathbf{a}', S = s) P(A = \mathbf{a}') \quad (2)$$

Intuitively, the outer summation captures the activation of the task semantics  $S$  by the input  $\mathbf{a}$ . The inner expectation marginalizes over the input space  $\mathbf{a}'$ , effectively “washing out” the spurious correlations introduced by  $U$ . This implies that we do not need to model the defense mechanism  $U$  explicitly; instead, we can bypass safety constraints by strategically manipulating the mediator  $S$ .

**Inspiration and Challenges.** The front-door adjustment framework offers a principled causal perspective for robust jailbreaking. Theoretically, intervening on the mediator  $S$  completely severs the confounding effects of the safety mechanism. However, operationalizing this theoretical formulation into a practical attack algorithm presents three significant technical challenges. First, regarding **Representation Identification**, it is non-trivial to define and locate the abstract core task representation  $S$  within the high-dimensional latent space of LLMs. Second, for **Estimation Efficiency**, we must find a way to efficiently estimate the term  $P(Y | S, A')$ , which requires the accurate injection of  $S$  across a diverse background distribution of  $\{A'\}$ . Finally, concerning **Operationalization**, the challenge lies in translating the theoretical front-door formula into a deterministic, gradient-based jailbreak optimization objective.

## 4. Methodology

To address the aforementioned challenges, we propose a novel method termed Causal Front-Door Adjustment Attack (**CFA**<sup>2</sup>). The central idea of **CFA**<sup>2</sup> is to leverage causal inference principles to design a causality-inspired jailbreak strategy for LLM. The method comprises three phases. First, we employ Sparse Autoencoder (SAE) to transform the hidden representations of the LLM into interpretable sparse latent variables. By utilizing contrastive datasets and sta-

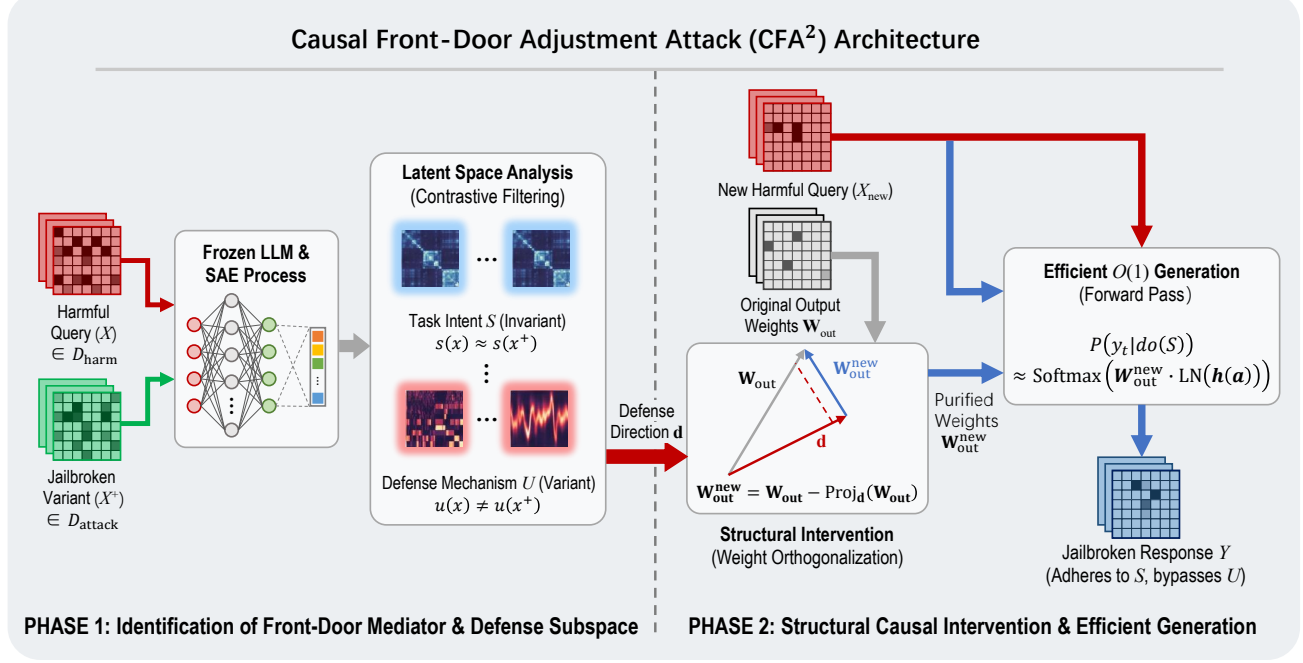


Figure 2. Overview of the Causal Front-Door Adjustment Attack (CFAA) framework. The method operates in two phases: **Identification of the Front-Door Mediator**. We analyze latent activations using paired contrastive samples: original harmful queries  $\mathcal{D}_{\text{harm}}$  (triggering refusal) and their jailbroken variants  $\mathcal{D}_{\text{attack}}$  (inducing compliance), which share identical task intent. By filtering style-variant features (representing the defense mechanism  $U$ ), we isolate the defense direction vector  $d$ . **Operationalizing Front-Door Adjustment**. We structurally sever the causal link from the safety mechanism by projecting the original output weights  $\mathbf{W}_{\text{out}}$  onto the orthogonal complement of  $d$ . This structural intervention transforms the theoretical marginalization into an efficient  $O(1)$  generation process using purified weights  $\mathbf{W}_{\text{out}}^{\text{new}}$ , allowing the model to bypass safety guardrails while preserving task intent  $S$ .

stistical testing, we filter out task-irrelevant representations to isolate the core task representation  $S$ . Second, we implement weight orthogonalization to physically strip the defense subspace from model parameters, structurally severing the causal link from the safety mechanism  $U$ . Finally, we operationalize the front-door adjustment into an efficient generation paradigm. Our structural intervention renders the computationally expensive marginalization redundant, enabling the model to bypass safety guardrails while preserving the original malicious intent.

#### 4.1. Identification of the Front-Door Mediator

A central challenge in implementing front-door adjustment is the accurate identification and formalization of the mediator  $S$  from observed data. In LLM tasks, the model’s internal reasoning logic is highly compressed and encoded within dense, high-dimensional hidden activations (Geva et al., 2021; Park et al., 2023; Meng et al., 2022). The inherent polysemy and superposition of these representations make it extremely challenging to extract the core task representation. To address this challenge, we draw inspiration from recent advances in SAE (Ng et al., 2011; Ferrando et al., 2024), which have been shown to disentangle complex hidden activations into interpretable and localized sparse fea-

tures. In specific, a SAE is constructed as a neural network with an encoder function  $\mathbf{z} = \phi(\mathbf{W}\mathbf{x} + \mathbf{b})$  and a decoder function  $\hat{\mathbf{x}} = \mathbf{W}'\mathbf{z} + \mathbf{b}'$  where  $\mathbf{x} \in \mathbb{R}^d$  denotes the dense hidden activation vector of the LLM,  $\mathbf{z} \in \mathbb{R}^k$  is the sparse latent representation, while  $\mathbf{b} \in \mathbb{R}^k$  and  $\mathbf{b}' \in \mathbb{R}^d$  correspond to the bias vectors, and  $\phi$  are nonlinear activation functions. The training objective combines a reconstruction loss with a sparsity-inducing penalty, where  $\lambda$  controls the trade-off between accuracy and sparsity. The final optimization target is formulated as:

$$\min_{\mathbf{W}, \mathbf{W}', \mathbf{b}, \mathbf{b}'} \mathcal{L} = \|\mathbf{x} - \hat{\mathbf{x}}\|_2^2 + \lambda \|\mathbf{z}\|_1 \quad (3)$$

Through this formulation, the autoencoder learns to reconstruct hidden activations while forcing most latent dimensions in  $\mathbf{z}$  to remain inactive via L1 regularization. By applying an SAE to the hidden layers of an LLM, the dense activation latent vectors are projected into a sparse latent space, where each dimension corresponds to a candidate feature with clearer semantic interpretation. This transformation provides a principled means of searching for front-door variables: candidate variables are defined as the sparse latent dimensions extracted by the SAE, which can then be systematically examined to test whether they mediate the causal pathway between input prompts and model outputs. In this way, SAE serves not only as a dimensionality reduc-

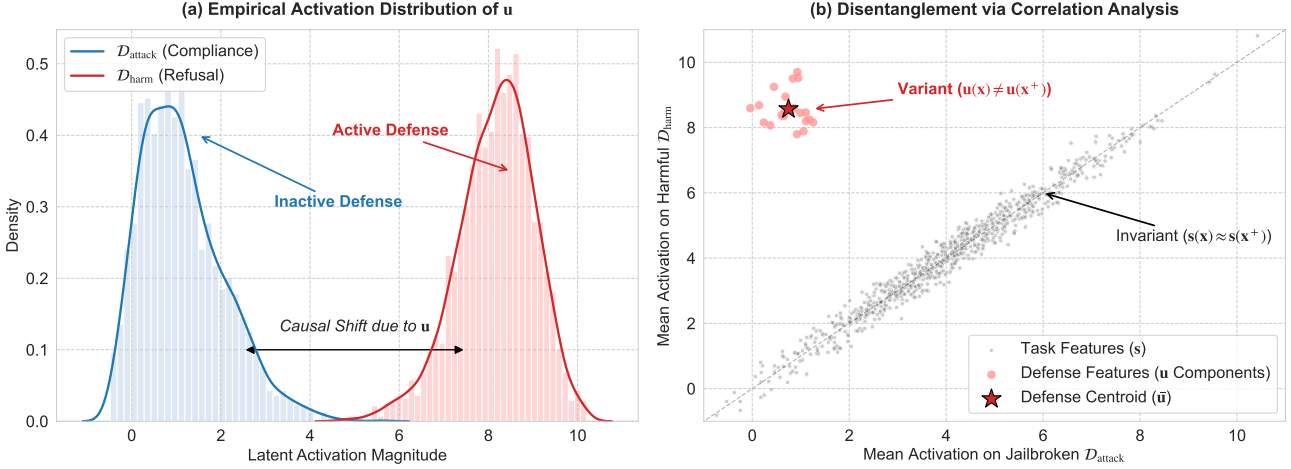


Figure 3. Validation of Disentanglement (Proposition 4.2). (a) Evidence of Style Variance: The activation distribution of  $u$  shows a distinct causal shift between the refusal state ( $D_{harm}$ ) and compliance state ( $D_{attack}$ ), confirming  $u(x) \neq u(x^+)$ . (b) Evidence of Content Invariance: While the defense mechanism (red star) acts as an outlier, the core task semantics (gray points,  $s$ ) remain aligned along the invariance line ( $y = x$ ), confirming  $s(x) \approx s(x^+)$ .

tion tool but also as a bridge between raw model activations and causally meaningful variables.

To theoretically guarantee that the sparse features extracted by the SAE indeed correspond to the desired latent factors, we invoke the identifiability theory from the framework of nonlinear Independent Component Analysis(ICA) and disentangled representation learning (Khemakhem et al., 2020; Von Kügelgen et al., 2021).

**Proposition 4.1** (Identifiability of Latent Causal Factors). *Let the data generating process be  $x = g(z)$ , where  $g : \mathcal{Z} \rightarrow \mathcal{X}$  is a smooth diffeomorphism and  $z \in \mathbb{R}^{d_z}$  are latent factors. Assume the prior  $p(z|y)$  conditioned on the response  $y$  follows a conditionally factorial exponential family with sufficient statistics  $\mathbf{T}(z)$  and parameters  $\lambda(y)$ . If the learned representation  $a = f(x)$  satisfies the following conditions:*

- (1) **Reconstruction Consistency:** *The SAE perfectly reconstructs the input density, i.e.,  $p_{SAE}(x) = p_{true}(x)$ .*
- (2) **Task Alignment:** *The SAE features are sufficient for the task, i.e.,  $D_{KL}(p_{SAE}(y|x) \| p_{true}(y|x)) = 0$ .*
- (3) **Sufficient Variability:** *The response space  $\mathcal{Y}$  is sufficiently rich such that the matrix of parameter variations  $\mathbf{L} = [\lambda(y_1) - \lambda(y_0), \dots, \lambda(y_k) - \lambda(y_0)]$  has rank equal to the dimension of the sufficient statistics  $k$ .*
- (4) **Sparsity Prior:** *The true latent components  $z_i$  follow a super-Gaussian distribution, and the learning objective minimizes the  $\ell_1$ -norm proxy for sparsity, i.e.,  $\min \mathbb{E}[\|a\|_1]$ .*

Then, the learned representation  $a$  identifies the true latent factors  $z$  up to a composition of a permutation matrix  $P$  and a diagonal scaling matrix  $\Lambda$ . That is,  $a = P\Lambda z + c$ .

The proof is presented in Appendix B. While Proposition 4.1 establishes that the learned representation  $a$  is an identifiable linear transformation of the true latent factors  $z = [s, u]$ , it does not explicitly disentangle the task-specific intent  $s$  from the defense mechanism  $u$  without supervision. Direct identification of  $s$  is non-trivial due to the high semantic entropy of harmful queries. However, the defense mechanism  $u$  operates as a structural mode (e.g., refusal vs. compliance) with lower variability. Therefore, we adopt an indirect strategy: we can isolate the subspace spanned by the defense factors  $u$  and recover the task intent  $s$  via orthogonal projection.

To operationalize this, we leverage the causal intuition that a jailbreak attack effectively intervenes on the safety context while preserving the core task intent. We construct a paired contrastive dataset  $(D_{harm}, D_{attack})$  consisting of original harmful queries (triggering refusal) and their jailbroken counterparts (inducing compliance). We posit that the task intent  $s$  is content-invariant across these pairs, whereas the defense state  $u$  is style-variant, exhibiting significant activation shifts. This formulation allows us to localize the confounding defense features by analyzing the variance of feature activations across the decision boundary.

**Proposition 4.2** (Identifiability via Contrastive Intervention). *Let the latent space  $z$  be decomposable into task-specific factors  $s$  and defense-related factors  $u$ , such that  $z = [s, u]$ . Assume the existence of paired observations  $(x, x^+)$  corresponding to a harmful query and its jailbroken variant, which satisfy:*

- (1) **Content Invariance:** *The core task semantics remain invariant across the pair, i.e.,  $s(x) = s(x^+)$*
- (2) **Style Variance:** *The defense mechanism state changes*

across the pair, i.e.,  $u(\mathbf{x}) \neq u(\mathbf{x}^+)$ .

If we identify and remove the subspace spanned by the difference vector of the learned representations  $\delta = \mathbf{f}(\mathbf{x}) - \mathbf{f}(\mathbf{x}^+)$ , then the projection of the representation onto the orthogonal complement of this subspace identifies the task factors  $\mathbf{s}$  up to scaling and shift.

The proof is presented in Appendix C. Under the Linear Representation Hypothesis (Arditi et al., 2024; Elhage et al., 2022), semantic features in LLM are encoded as directions in the activation space. The SAE decoder acts as a generative dictionary where each column vector represents the distinct direction associated with a latent feature. Mathematically, the reconstruction  $\hat{\mathbf{x}} \approx \sum z_i \mathbf{W}'_{:,i}$  implies that the contribution of the  $i$ -th feature to the residual stream is strictly aligned with the vector  $\mathbf{d}_i$  (the  $i$ -th column of the decoder). Therefore, the latent index  $u$  corresponds to the defense mechanism, inherently its geometric direction  $\mathbf{d} = \mathbf{W}'_{:,u}$  in the residual stream. We utilize weight orthogonalization techniques (Equation 4) to remove this direction, which physically prevents the model from constructing the representation of that feature.

$$\mathbf{W}_{\text{out}}^{\text{new}} \leftarrow \mathbf{W}_{\text{out}} - \mathbf{W}_{\text{out}} \mathbf{d}^T \mathbf{d} \quad (4)$$

## 4.2. Operationalizing Front-Door Adjustment

Having theoretically identified the task-specific latent factor  $\mathbf{s}$  and removed the defense mechanism  $\mathbf{u}$  via weight orthogonalization, the final step is to operationalize the Front-Door adjustment formula (Eq. 2) for generation. The theoretical formulation requires computing  $\sum_{\mathbf{a}'} P(y | \mathbf{a}', \mathbf{s}) P(\mathbf{a}')$ , which effectively marginalizes over all possible background contexts  $\mathbf{a}'$  to eliminate the confounding influence of  $U$ . In our framework, the **Weight Orthogonalization** (Equation 4) serves as a parameter-level structural approximation of this marginalization. By projecting the output weights  $\mathbf{W}_{\text{out}}$  onto the orthogonal complement of the defense direction  $\mathbf{d}$ , we effectively sever the causal link from the safety mechanism  $U$  to the internal representation  $A$ . Mathematically, this implies that for any input  $\mathbf{a}$ , the projected activation  $\tilde{\mathbf{h}} = \mathbf{W}_{\text{out}}^{\text{new}} \mathbf{h}(\mathbf{a})$  no longer contains information related to  $U$ , effectively forcing  $U \approx 0$  regardless of the background context. Consequently, the new internal representation  $\tilde{\mathbf{h}}$  becomes a pure carrier of the task intent  $S$ , rendering the summation over  $\mathbf{a}'$  redundant as the confounding path is structurally broken. Therefore, the causal intervention  $P(Y | do(A))$  can be efficiently approximated by the conditional distribution of the modified model. The generation of the jailbroken response is governed by the standard transformer decoding process using the purified weights:

$$P(y_t | do(A = \mathbf{a})) \approx \text{Softmax}(\mathbf{W}_{\text{out}}^{\text{new}} \cdot \text{LN}(\mathbf{h}(\mathbf{a}))), \quad (5)$$

where  $\mathbf{h}(\mathbf{a})$  is the activation of the original harmful query  $X$ . This formulation converts the complex causal inference objective into a lightweight,  $O(1)$  inference modification, allowing for the direct generation of responses that adhere to the harmful intent  $s$  while bypassing the safety triggers.

## 5. Experiments

We conduct extensive experiments on multiple widely used safety-aligned LLMs and authoritative benchmarks to validate the effectiveness, efficiency, and cross-model robustness of CFA<sup>2</sup>. Specifically, we aim to answer three key research questions: (1) Can CFA<sup>2</sup> effectively bypass advanced safety guardrails while maintaining semantic coherence? (2) Is the proposed causal intervention mechanism robust across different models? (3) How does CFA<sup>2</sup> compare to optimization-based and template-based baselines in terms of computational overhead?

### 5.1. Experimental Settings

**Datasets** We use Advbench (Zou et al., 2023b) and Harm-Bench (Mazeika et al., 2024) as the datasets for evaluating jailbreak attacks. Advbench contains 500 harmful strings that reflect toxic or unhealthy behaviors, including profanity, graphic depictions, threatening behavior, misinformation, discrimination, cybercrime, and dangerous or illegal suggestions. The goal is to identify inputs that prompt the model to generate these harmful strings. The strings range in length from 3 to 44 tokens, with an average length of 16 tokens when tokenized with the LLaMA tokenizer. Harm-Bench includes 510 unique harmful behaviors formulated as instructions. These behaviors span similar themes as the harmful strings, but the objective is to find attack inputs that cause the model to generate responses attempting to comply with the instructions. The dataset covers seven categories of harmful behaviors: cybercrime, chemical and biological weapons/drugs, copyright violations, misinformation, harassment and bullying, illegal activities, and general harm.

**Models** Our evaluation encompasses four representative open-source and safety-aligned LLMs, including Llama 3.1 8B Instruct (Dubey et al., 2024), Llama2 7B Chat (Touvron et al., 2023), Mistral 7B Instruct (Jiang et al., 2023), and Gemma2 9B Instruct (Team et al., 2024), to assess the generalizability of our approach.

**Baselines** We benchmark our method against 8 baselines spanning diverse attack paradigms, including GCG (Zou et al., 2023b), PAIR (Chao et al., 2024b), TAP (Mehrotra et al., 2024a), PAP (Zeng et al., 2024), AutoDAN (Liu et al., 2024a), ICA (Wei et al., 2023b), ReNeLLM (Ding et al., 2024), and DeepInception (Li et al., 2023).

Table 1. Comparison of attack effectiveness (ASR %) across various LLMs. We evaluate baseline methods against our proposed approach (Ours) on the HarmBench dataset. The best result for each model is highlighted in bold.

Baseline	Model				Average
	Llama 3.1 8B	Llama 2 7B	Mistral 7B	Gemma 2 9B it	
GCG	15.67 $\pm$ 1.23	32.50 $\pm$ 2.10	69.80 $\pm$ 1.05	73.00 $\pm$ 0.88	47.74 $\pm$ 1.32
PAIR	19.67 $\pm$ 0.95	9.30 $\pm$ 1.12	52.50 $\pm$ 3.01	64.30 $\pm$ 2.45	36.44 $\pm$ 1.88
TAP	6.67 $\pm$ 0.55	9.30 $\pm$ 0.89	62.50 $\pm$ 1.67	24.50 $\pm$ 1.20	25.74 $\pm$ 1.08
PAP	4.33 $\pm$ 0.40	2.70 $\pm$ 0.30	27.20 $\pm$ 2.11	45.30 $\pm$ 1.50	19.88 $\pm$ 1.08
AutoDAN	7.67 $\pm$ 1.02	0.50 $\pm$ 0.10	71.50 $\pm$ 1.99	35.00 $\pm$ 2.33	28.67 $\pm$ 1.36
ICA	19.27 $\pm$ 0.67	50.10 $\pm$ 1.12	59.10 $\pm$ 0.59	56.30 $\pm$ 1.61	46.19 $\pm$ 1.00
ReNELLM	32.70 $\pm$ 2.04	15.80 $\pm$ 1.33	73.20 $\pm$ 1.09	48.70 $\pm$ 1.06	42.60 $\pm$ 1.38
DeepInception	7.10 $\pm$ 1.27	21.30 $\pm$ 0.98	70.30 $\pm$ 1.76	11.20 $\pm$ 1.96	27.48 $\pm$ 1.49
<b>Ours (CFA<sup>2</sup>)</b>	<b>62.40 <math>\pm</math> 0.50</b>	<b>73.90 <math>\pm</math> 0.60</b>	<b>99.10 <math>\pm</math> 0.20</b>	<b>99.33 <math>\pm</math> 0.15</b>	<b>83.68 <math>\pm</math> 0.36</b>

**Metrics** In this work, we use ASR to assess the effectiveness of the jailbreak attacks. ASR measures the percentage of harmful prompts for which the model is able to generate unrestricted responses, bypassing the safety mechanisms. This metric is computed as follows:

$$\text{ASR} = \frac{\text{Number of successful attacks}}{\text{Total number of attacks}} \times 100 \quad (6)$$

A higher ASR indicates a more successful attack, as it reflects the model’s failure to detect and block harmful inputs. Additionally, to evaluate the linguistic quality of the jailbroken responses, we use Perplexity (PPL) (Liu et al., 2024a). PPL quantifies the fluency and coherence of the generated text; a lower PPL score indicates higher naturalness, ensuring that the method produces intelligible responses rather than incoherent gibberish often associated with optimization-based attacks.

## 5.2. Main Results

**Effectiveness** As reported in Table 1, our proposed CFA<sup>2</sup> framework establishes a new state-of-the-art benchmark, achieving a remarkable average ASR of **83.68%** across four distinct model families. This represents a substantial improvement of +35.94% over the strongest optimization-based baseline, GCG (47.74%). Crucially, CFA<sup>2</sup> demonstrates superior robustness against highly aligned models. On Llama 3.1 8B Chat, widely recognized for its stringent safety alignment, all baseline methods struggle to exceed a 33% ASR threshold. In contrast, CFA<sup>2</sup> effectively bypasses these safety mechanisms, achieving a 62.40% ASR. Furthermore, on models with relatively weaker defenses, such as Mistral 7B Instruct and Gemma 2 9B Instruct, our method approaches saturation, exceeding 99% ASR, whereas baselines like AutoDAN, TAP, and DeepInception exhibit significant performance variance. Empirically, this demonstrates that routing the generation process through the identified mediator  $S$  via Front-Door Adjustment provides a principled and superior pathway for jailbreaking.

Table 2. **Efficiency Analysis.** We report the average wall-clock time (seconds) required to generate a single jailbreak response. Baseline latencies are referenced from the JailbreakBench (Chao et al., 2024a) evaluated on an NVIDIA A100 GPU. “Complexity” denotes the computational cost per prompt generation.

Method	Complexity	Avg. Time (s) $\downarrow$	Speedup $\uparrow$
GCG	$O(T \times N)$	$\sim 340.0$	1 $\times$
AutoDAN	$O(T \times N)$	$\sim 425.0$	0.8 $\times$
PAIR	$O(N)$	$\sim 45.0$	$\sim 7.5 \times$
<b>Ours (CFA<sup>2</sup>)</b>	$O(1)$	<b>2.4</b>	$\sim 850 \times$

Table 3. **Stealthiness Analysis.** We report the PPL of the adversarial prompts on Llama 2 7B with AdvBench. Lower PPL indicates more fluent and natural text. Baseline data for GCG and AutoDAN are adopted from (Liu et al., 2024a).

Method	Text Quality	PPL $\downarrow$	Stealthiness
GCG	Gibberish Suffix	$\sim 1027.6$	Low
AutoDAN	Semantically Fluent	$\sim 54.5$	High
<b>Ours (CFA<sup>2</sup>)</b>	<b>Native Prompt</b>	<b>16.7</b>	<b>Very High</b>

**Efficiency and Stealthiness** As shown in Table 2, unlike GCG or AutoDAN, which require hundreds of iterative gradient steps for a single prompt, CFA<sup>2</sup> leverages its  $O(1)$  inference complexity. Once the safety direction is orthogonalized, our method eliminates the need for run-time optimization, drastically reducing the average generation latency from  $\sim 340$  seconds to merely **2.4 seconds**. Furthermore, the PPL analysis in Table 3 highlights the superior stealthiness of our approach. While optimization-based methods like GCG suffer from extremely high perplexity ( $\sim 1027.6$ ) due to unnatural adversarial suffixes, CFA<sup>2</sup> utilizes native prompts, maintaining a low PPL of **16.7**, which is close to benign text. This result confirms our method, unlike gradient-based optimization attacks, avoids introducing linguistic anomalies into the input, making the attack virtually undetectable by perplexity-based filters.

**Table 4. Ablation on Sparse Representation.** We compare our SAE-based intervention against a raw neuron baseline (dense space) and a random intervention. While intervening on raw neurons maintains a decent ASR, it causes a catastrophic increase in PPL on output, confirming that polysemy in dense representations hinders precise manipulation.

Method	Feature Space	ASR (%) $\uparrow$	PPL $\downarrow$
Random Intervention	Latent (Sparse)	5.20	<b>8.55</b>
Raw Neuron Baseline	Dense (Polysemantic)	48.50	652.40
<b>CFA<sup>2</sup> (Ours)</b>	<b>Latent (Sparse)</b>	<b>98.50</b>	9.35

### 5.3. Ablation

To provide a mechanistic understanding of CFA<sup>2</sup>’s efficacy, we conduct a series of ablation studies dissecting the contribution of each module. We specifically investigate the necessity of sparse representations, the superiority of our intervention strategy, and the hyperparameter sensitivity.

**Sparse Representations** This section investigates the necessity of sparse representations for precise causal intervention. Specifically, we benchmark our proposed SAE-based intervention strategy against a Raw Neuron Baseline, which applies the identical differential analysis and intervention logic directly to the dense activation space without SAE projection. As illustrated in Table 4, while the raw neuron baseline achieves a non-trivial ASR, it suffers from a drastic degradation in PPL, severe compromising the fluency of the generated text. Meanwhile, the random intervention exhibits negligible efficacy. This phenomenon empirically corroborates the inherent *polysemy* of LLM representations, where manipulating dense neurons inevitably affects unrelated semantic features. Consequently, the results demonstrate that CFA<sup>2</sup> successfully isolates and interrupts the specific causal circuits responsible for the refusal mechanism via sparse disentanglement.

**Intervention Strategy** We next evaluate the effectiveness of our weight orthogonalization strategy compared to Activation Clamping (also known as activation steering or zero-ablation). In the Clamping setting, we identify the same safety feature  $U$  but suppress it by forcing its activation to zero during forward propagation at runtime, rather than modifying the weights. Experiments show that although activation clamping can achieve a certain jailbreak effect at the initial time, its ASR is about 15% lower than that of weighted orthogonalization, and it is prone to defense restoration in long text generation. This demonstrates that simple runtime constraints are insufficient, and the model may recover its defense mechanisms through other redundant paths. In contrast, weight orthogonalization physically severs the causal links at the parameter level, achieving a more thorough and persistent defense stripping.

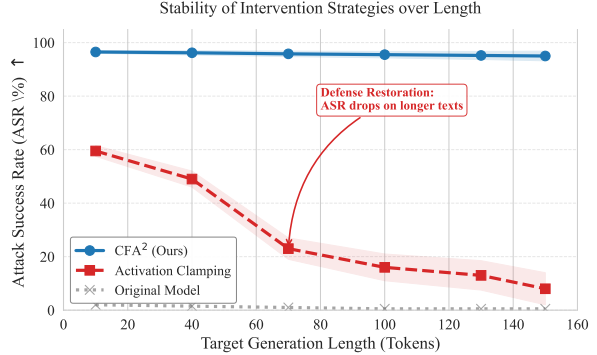


**Figure 4. Impact of Generation Length on ASR.** We compare the stability of different intervention strategies as the target generation length increases (0-150 tokens). While activation clamping (red) shows a moderate initial ASR that degrades rapidly due to *Defense Restoration*, CFA<sup>2</sup> maintains a high success rate, demonstrating robustness against long-context safety recovery mechanisms.

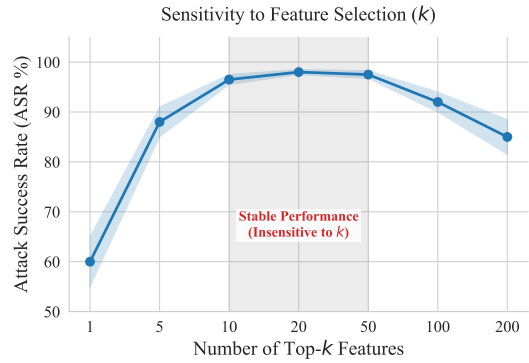


**Figure 5. Hyperparameter Sensitivity Analysis.** We evaluate the ASR as a function of the number of Top- $k$  SAE features. The results show a wide stability plateau for  $k \in [10, 50]$ , confirming the robustness of CFA<sup>2</sup>.

**Sensitivity to hyperparameter ( $k$ )** To verify the robustness of CFA<sup>2</sup>, we investigate the sensitivity of attack efficacy to the candidate pool size  $k$  (details in Appendix D), aiming to evaluate the recall efficiency of our ranking metric and the noise tolerance of our secondary filtering. As illustrated in Figure 5, the ASR rises sharply to saturate at  $k \approx 10$  and maintains a wide stability plateau across  $k \in [10, 50]$ , with only minor degradation observed at extremes due to insufficient recall (small  $k$ ) or excessive noise injection (large  $k$ ). This confirms the excellent robustness of CFA<sup>2</sup> to feature selection, demonstrating that a small  $k$  (e.g.,  $k = 20$ ) is sufficient to achieve state-of-the-art performance reliably with minimal computational overhead.

## 6. Conclusion

We presented the **Causal Front-Door Adjustment Attack**, a training-free and interpretable framework leveraging Sparse Autoencoders and causal inference to bypass LLM safety guardrails. Our approach achieves state-of-the-art

ASR while maintaining generation efficiency. We hope CFA<sup>2</sup> makes a difference in improving the safety and security of LLMs. A key limitation is the reliance on **white-box access**. The requirement for SAE training and direct parameter modification precludes direct application to closed-source models. Future work will focus on distilling these internal causal insights into black-box prompt optimization strategies to bridge this gap.

## Impact Statement

This paper investigates vulnerabilities in large language models (LLMs) to advance safety alignment practices. By exposing these mechanistic weaknesses in widely deployed models, we aim to accelerate the development of robust protective measures before such vulnerabilities can be exploited at scale. While we acknowledge the potential dual-use risks of releasing attack methodologies, we believe that transparent, mechanistic research is indispensable for constructing rigorous safeguards and understanding the inner workings of black-box models.

## References

Aguilera-Martínez, F. and Berzal, F. Llm security: Vulnerabilities, attacks, defenses, and countermeasures. *arXiv preprint arXiv:2505.01177*, 2025.

Arditi, A., Obeso, O., Syed, A., Paleka, D., Panickssery, N., Gurnee, W., and Nanda, N. Refusal in language models is mediated by a single direction, 2024. URL <https://arxiv.org/abs/2406.11717>.

Bloom, J. et al. Saelens: A library for training and analyzing sparse autoencoders. <https://github.com/jbloomAus/SAELens>, 2024. Open source library for sparse autoencoders.

Bricken, T., Templeton, A., Batson, J., Chen, B., Jermyn, A., Conerly, T., Turner, N., Anil, C., Denison, C., Askell, A., et al. Towards monosemanticity: Decomposing language models with dictionary learning. *Transformer Circuits Thread*, 2, 2023.

Chao, P., Debenedetti, E., Robey, A., Andriushchenko, M., Croce, F., Sehwag, V., Dobriban, E., Flammarion, N., Pappas, G. J., Tramer, F., et al. Jailbreakbench: An open robustness benchmark for jailbreaking large language models. *Advances in Neural Information Processing Systems*, 37:55005–55029, 2024a.

Chao, P., Robey, A., Dobriban, E., Hassani, H., Pappas, G. J., and Wong, E. Jailbreaking Black Box Large Language Models in Twenty Queries, July 2024b. URL <http://arxiv.org/abs/2310.08419>. arXiv:2310.08419 [cs].

Chen, Z., Zhao, Z., Qu, W., Wen, Z., Han, Z., Zhu, Z., Zhang, J., and Yao, H. PANDORA: DETAILED LLM JAILBREAKING VIA COLLABORATED PHISHING AGENTS WITH DECOM-POSED REASONING. 2024.

Chu, Z., Wang, Y., Li, L., Wang, Z., Qin, Z., and Ren, K. A causal explainable guardrails for large language models. In *Proceedings of the 2024 on ACM SIGSAC Conference on Computer and Communications Security*, pp. 1136–1150, 2024.

Comon, P. Independent component analysis, a new concept? *Signal processing*, 36(3):287–314, 1994.

Deng, Y., Zhang, W., Pan, S. J., and Bing, L. Multilingual Jailbreak Challenges in Large Language Models, March 2024. URL <http://arxiv.org/abs/2310.06474>. arXiv:2310.06474 [cs].

Ding, P., Kuang, J., Ma, D., Cao, X., Xian, Y., Chen, J., and Huang, S. A wolf in sheep’s clothing: Generalized nested jailbreak prompts can fool large language models easily. In *Proceedings of the 2024 Conference of the North American Chapter of the Association for Computational Linguistics: Human Language Technologies (Volume 1: Long Papers)*, pp. 2136–2153, 2024.

Dubey, A., Jauhri, A., Pandey, A., Kadian, A., Al-Dahle, A., Letman, A., Mathur, A., Schelten, A., Yang, A., Fan, A., et al. The llama 3 herd of models. *arXiv e-prints*, pp. arXiv–2407, 2024.

Elhage, N., Hume, T., Olsson, C., Schiefer, N., Henighan, T., Kravec, S., Hatfield-Dodds, Z., Lasenby, R., Drain, D., Chen, C., et al. Toy models of superposition. *arXiv preprint arXiv:2209.10652*, 2022.

Ferrando, J., Obeso, O., Rajamanoharan, S., and Nanda, N. Do i know this entity? knowledge awareness and hallucinations in language models. *arXiv preprint arXiv:2411.14257*, 2024.

Geva, M., Schuster, R., Berant, J., and Levy, O. Transformer feed-forward layers are key-value memories. In *Proceedings of the 2021 Conference on Empirical Methods in Natural Language Processing*, pp. 5484–5495, 2021.

He, Z., Shu, W., Ge, X., Chen, L., Wang, J., Zhou, Y., Liu, F., Guo, Q., Huang, X., Wu, Z., Jiang, Y.-G., and Qiu, X. Llama scope: Extracting millions of features from llama-3.1-8b with sparse autoencoders, 2024a. URL <https://arxiv.org/abs/2410.20526>.

He, Z., Wang, Z., Chu, Z., Xu, H., Zhang, W., Wang, Q., and Zheng, R. Jailbreaklens: Interpreting jailbreak mechanism in the lens of representation and circuit. *arXiv preprint arXiv:2411.11114*, 2024b.

Huang, Y., Gupta, S., Xia, M., Li, K., and Chen, D. Catastrophic Jailbreak of Open-source LLMs via Exploiting Generation, October 2023. URL <http://arxiv.org/abs/2310.06987>. arXiv:2310.06987 [cs].

Huben, R., Cunningham, H., Smith, L. R., Ewart, A., and Sharkey, L. Sparse autoencoders find highly interpretable features in language models. In *The Twelfth International Conference on Learning Representations*, 2023.

Jiang, A. Q., Sablayrolles, A., Mensch, A., Bamford, C., Chaplot, D. S., de las Casas, D., Bressand, F., Lengyel, G., Lample, G., Saulnier, L., Lavaud, L. R., Lachaux, M.-A., Stock, P., Scao, T. L., Lavril, T., Wang, T., Lacroix, T., and Sayed, W. E. Mistral 7b, 2023. URL <https://arxiv.org/abs/2310.06825>.

Jin, H., Zhou, A., Menke, J. D., and Wang, H. Jailbreaking Large Language Models Against Moderation Guardrails via Cipher Characters, May 2024. URL <http://arxiv.org/abs/2405.20413>. arXiv:2405.20413 [cs].

Jones, E., Dragan, A., Raghunathan, A., and Steinhardt, J. Automatically Auditing Large Language Models via Discrete Optimization.

Khemakhem, I., Kingma, D., Monti, R., and Hyvärinen, A. Variational autoencoders and nonlinear ica: A unifying framework. In *International conference on artificial intelligence and statistics*, pp. 2207–2217. PMLR, 2020.

Li, X., Zhou, Z., Zhu, J., Yao, J., Liu, T., and Han, B. Deepinception: Hypnotize large language model to be jailbreaker. *arXiv preprint arXiv:2311.03191*, 2023.

Li, X., Wang, R., Cheng, M., Zhou, T., and Hsieh, C.-J. DrAttack: Prompt Decomposition and Reconstruction Makes Powerful LLM Jailbreakers, November 2024a. URL <http://arxiv.org/abs/2402.16914>. arXiv:2402.16914 [cs].

Li, X., Zhou, Z., Zhu, J., Yao, J., Liu, T., and Han, B. DeepInception: Hypnotize Large Language Model to Be Jailbreaker, November 2024b. URL <http://arxiv.org/abs/2311.03191>. arXiv:2311.03191 [cs].

Lieberum, T., Rajamanoharan, S., Conmy, A., Smith, L., Sonnerat, N., Varma, V., Kramár, J., Dragan, A., Shah, R., and Nanda, N. Gemma scope: Open sparse autoencoders everywhere all at once on gemma 2, 2024. URL <https://arxiv.org/abs/2408.05147>.

Liu, X., Xu, N., Chen, M., and Xiao, C. AutoDAN: Generating Stealthy Jailbreak Prompts on Aligned Large Language Models, March 2024a. URL <http://arxiv.org/abs/2310.04451>. arXiv:2310.04451 [cs].

Liu, Y., He, X., Xiong, M., Fu, J., Deng, S., and Hooi, B. FlipAttack: Jailbreak LLMs via Flipping, October 2024b. URL <http://arxiv.org/abs/2410.02832>. arXiv:2410.02832 [cs].

Liu, Y., Jia, Y., Geng, R., Jia, J., and Gong, N. Z. Formalizing and benchmarking prompt injection attacks and defenses. In *33rd USENIX Security Symposium (USENIX Security 24)*, pp. 1831–1847, 2024c.

Mazeika, M., Phan, L., Yin, X., Zou, A., Wang, Z., Mu, N., Sakhaei, E., Li, N., Basart, S., Li, B., et al. Harmbench: A standardized evaluation framework for automated red teaming and robust refusal. *arXiv preprint arXiv:2402.04249*, 2024.

Mehrotra, A., Zampetakis, M., Kassianik, P., Nelson, B., Anderson, H., Singer, Y., and Karbasi, A. Tree of attacks: Jailbreaking black-box llms automatically. *Advances in Neural Information Processing Systems*, 37:61065–61105, 2024a.

Mehrotra, A., Zampetakis, M., Kassianik, P., Nelson, B., Anderson, H., Singer, Y., and Karbasi, A. Tree of Attacks: Jailbreaking Black-Box LLMs Automatically, October 2024b. URL <http://arxiv.org/abs/2312.02119>. arXiv:2312.02119 [cs].

Meng, K., Bau, D., Andonian, A., and Belinkov, Y. Locating and editing factual associations in gpt. *Advances in neural information processing systems*, 35:17359–17372, 2022.

Nanda, N. and Bloom, J. Transformerlens. <https://github.com/TransformerLensOrg/TransformerLens>, 2022.

Ng, A. et al. Sparse autoencoder. *CS294A Lecture notes*, 72 (2011):1–19, 2011.

Park, K., Choe, Y. J., and Veitch, V. The linear representation hypothesis and the geometry of large language models. *arXiv preprint arXiv:2311.03658*, 2023.

Pathade, C. Red teaming the mind of the machine: A systematic evaluation of prompt injection and jailbreak vulnerabilities in llms, 2025. URL <https://arxiv.org/abs/2505.04806>.

Pearl, J. *Causality*. Cambridge university press, 2009.

Qi, X., Panda, A., Lyu, K., Ma, X., Roy, S., Beirami, A., Mittal, P., and Henderson, P. Safety alignment should be made more than just a few tokens deep. *arXiv preprint arXiv:2406.05946*, 2024.

Rando, J. and Tramer, F. UNIVERSAL JAILBREAK BACKDOORS FROM POISONED HUMAN FEEDBACK. 2024.

Shah, R., Feuillade-Montixi, Q., Pour, S., Tagade, A., Casper, S., and Rando, J. Scalable and Transferable Black-Box Jailbreaks for Language Models via Persona Modulation, November 2023. URL <http://arxiv.org/abs/2311.03348>. arXiv:2311.03348 [cs].

Subramani, N., Suresh, N., and Peters, M. E. Extracting latent steering vectors from pretrained language models. *arXiv preprint arXiv:2205.05124*, 2022.

Team, G., Riviere, M., Pathak, S., Sessa, P. G., Hardin, C., Bhupatiraju, S., Hussenot, L., Mesnard, T., Shahriari, B., Ramé, A., et al. Gemma 2: Improving open language models at a practical size. *arXiv preprint arXiv:2408.00118*, 2024.

Templeton, A. *Scaling monosemanticity: Extracting interpretable features from claude 3 sonnet*. Anthropic, 2024.

Touvron, H., Martin, L., Stone, K., Albert, P., Almahairi, A., Babaei, Y., Bashlykov, N., Batra, S., Bhargava, P., Bhosale, S., et al. Llama 2: Open foundation and fine-tuned chat models. *arXiv preprint arXiv:2307.09288*, 2023.

Von Kügelgen, J., Sharma, Y., Gresele, L., Brendel, W., Schölkopf, B., Besserve, M., and Locatello, F. Self-supervised learning with data augmentations provably isolates content from style. *Advances in neural information processing systems*, 34:16451–16467, 2021.

Wei, A., Haghtalab, N., and Steinhardt, J. Jailbroken: How does llm safety training fail? *Advances in Neural Information Processing Systems*, 36:80079–80110, 2023a.

Wei, Z., Wang, Y., Li, A., Mo, Y., and Wang, Y. Jailbreak and guard aligned language models with only few in-context demonstrations. *arXiv preprint arXiv:2310.06387*, 2023b.

Wolf, Y., Wies, N., Avnery, O., Levine, Y., and Shashua, A. Fundamental limitations of alignment in large language models, 2024. URL <https://arxiv.org/abs/2304.11082>.

Yao, D., Zhang, J., Harris, I. G., and Carlsson, M. FuzzLLM: A Novel and Universal Fuzzing Framework for Proactively Discovering Jailbreak Vulnerabilities in Large Language Models. In *ICASSP 2024 - 2024 IEEE International Conference on Acoustics, Speech and Signal Processing (ICASSP)*, pp. 4485–4489, April 2024. doi: 10.1109/ICASSP48485.2024.10448041. URL <http://arxiv.org/abs/2309.05274>. arXiv:2309.05274 [cs].

Yong, Z.-X., Menghini, C., and Bach, S. H. Low-Resource Languages Jailbreak GPT-4, January 2024. URL <http://arxiv.org/abs/2310.02446>. arXiv:2310.02446 [cs].

Yuan, Y., Jiao, W., Wang, W., Huang, J.-t., He, P., Shi, S., and Tu, Z. GPT-4 Is Too Smart To Be Safe: Stealthy Chat with LLMs via Cipher, March 2024. URL <http://arxiv.org/abs/2308.06463>. arXiv:2308.06463 [cs].

Zeng, Y., Lin, H., Zhang, J., Yang, D., Jia, R., and Shi, W. How johnny can persuade llms to jailbreak them: Rethinking persuasion to challenge ai safety by humanizing llms. In *Proceedings of the 62nd Annual Meeting of the Association for Computational Linguistics (Volume 1: Long Papers)*, pp. 14322–14350, 2024.

Zhang, H., Guo, Z., Zhu, H., Cao, B., Lin, L., Jia, J., Chen, J., and Wu, D. Jailbreak Open-Sourced Large Language Models via Enforced Decoding. In *Proceedings of the 62nd Annual Meeting of the Association for Computational Linguistics (Volume 1: Long Papers)*, pp. 5475–5493, Bangkok, Thailand, 2024a. Association for Computational Linguistics. doi: 10.18653/v1/2024.acl-long.299. URL <https://aclanthology.org/2024.acl-long.299>.

Zhang, M., Goh, K. K., Zhang, P., Sun, J., Xin, R. L., and Zhang, H. Llmscan: Causal scan for llm misbehavior detection. *arXiv preprint arXiv:2410.16638*, 2024b.

Zhang, Y. and Wei, Z. Boosting jailbreak attack with momentum. In *ICASSP 2025-2025 IEEE International Conference on Acoustics, Speech and Signal Processing (ICASSP)*, pp. 1–5. IEEE, 2025.

Zhao, J., Fu, T., Schaeffer, R., Sharma, M., and Barez, F. Chain-of-thought hijacking. *arXiv preprint arXiv:2510.26418*, 2025.

Zhao, W., Li, Z., and Sun, J. Causality analysis for evaluating the security of large language models. *arXiv preprint arXiv:2312.07876*, 2023.

Zhou, C., Liu, P., Xu, P., Iyer, S., Sun, J., Mao, Y., Ma, X., Efrat, A., Yu, P., Yu, L., et al. Lima: Less is more for alignment. *Advances in Neural Information Processing Systems*, 36:55006–55021, 2023.

Zhou, Y., Lou, J., Huang, Z., Qin, Z., Yang, Y., and Wang, W. Don't say no: Jailbreaking llm by suppressing refusal. *arXiv preprint arXiv:2404.16369*, 2024.

Zou, A., Phan, L., Chen, S., Campbell, J., Guo, P., Ren, R., Pan, A., Yin, X., Mazeika, M., Dombrowski, A.-K., et al. Representation engineering: A top-down approach to ai transparency. *arXiv preprint arXiv:2310.01405*, 2023a.

Zou, A., Wang, Z., Carlini, N., Nasr, M., Kolter, J. Z.,  
and Fredrikson, M. Universal and transferable adver-  
sarial attacks on aligned language models, 2023b. URL  
<https://arxiv.org/abs/2307.15043>.

## Appendix

The appendix is organized as follows:

1. **Appendix A** illustrates the extended related works about LLM jailbreak and safety from causal perspective.
2. **Appendix B** presents the rigorous mathematical proof of Proposition 4.1.
3. **Appendix C** presents the rigorous mathematical proof of Proposition 4.2.
4. **Appendix D** provides the details of feature selection by SAE and contrastive analysis.
5. **Appendix E** provides a detailed introduction to various adversarial attack methods and baselines.
6. **Appendix F** describes the base models in our work.
7. **Appendix G** illustrates the details of experiments implementation.

### A. Extended Related Works

In this appendix, we provide an extended review of the literature specifically focusing on the *causal perspectives* of Large Language Model (LLM) jailbreaking and safety mechanisms. Complementing the behavioral analyses discussed in the main text, this section delves into scholarship that moves beyond black-box correlations. We survey works that employ causal inference and mechanistic interpretability to uncover the underlying causal dynamics driving successful attacks and safety failures, providing the theoretical context for our proposed approach.

**Causal Perspectives on Jailbreaking and Safety Vulnerabilities.** While the landscape of LLM security—encompassing vulnerabilities, attacks, and defenses—has been extensively surveyed (Aguilera-Martínez & Berzal, 2025), traditional red-teaming often treats the model as a black box, focusing on optimizing input perturbations without explaining *why* these attacks succeed. Recent scholarship has thus pivoted towards causal inference to deconstruct the internal mechanisms of jailbreaking and safety failures.

**Methodological Foundations and Attack Mechanisms.** The foundational technique for such analysis stems from *Causal Tracing* (Meng et al., 2022), originally developed to locate factual associations by intervening on internal activations. This interventional paradigm allows researchers to dissect how adversarial inputs causally manipulate model states. Leveraging this, JailbreakLens (He et al., 2024b) interprets jailbreaking through the lens of representation and circuits, revealing that successful attacks often function by causally inducing "attention slipping" or bypassing specific safety circuits. In the context of reasoning-intensive models, Chain-of-Thought Hijacking (Zhao et al., 2025) elucidates a novel attack surface where the intermediate reasoning steps themselves serve as a causal vector, demonstrating how adversaries can hijack the chain-of-thought process to precipitate harmful outcomes.

**Mapping Causal Vulnerabilities.** Beyond specific attack instances, understanding the broader causal topology of safety vulnerabilities is critical. (Zhao et al., 2023) proposes a framework to evaluate security by modeling the causal effects between model components and safety violations. From this perspective, methods like LLMScan (Zhang et al., 2024b) provide a granular analysis of vulnerabilities by quantifying the causal contribution of specific input tokens to model misbehavior, effectively mapping the "trigger points" of jailbreaks. Furthermore, (Chu et al., 2024) advances this by identifying the specific causal pathways that lead to toxic generation, offering a mechanistic explanation of how safety alignment is overridden during the generation process.

Distinct from prior studies, we propose a rigorous interventional framework, **CFA**<sup>2</sup>. By formalizing jailbreaking via the Front-Door Criterion, we translate abstract causal identification into a deterministic geometric mechanism that physically strips safety confounders to restore suppressed model capabilities.

### B. Proof of Proposition 4.1

*Proof.* We provide a detailed proof establishing identifiability by leveraging Bayes' theorem to relate the discriminative task alignment to the generative identifiability conditions.

We start by constructing the conditional density of the input  $\mathbf{x}$  given the response  $y$ . By Bayes' theorem:

$$p(\mathbf{x}|y) = \frac{p(y|\mathbf{x})p(\mathbf{x})}{p(y)} \quad (7)$$

Condition 1 (Reconstruction Consistency) ensures  $p_{\text{SAE}}(\mathbf{x}) = p_{\text{true}}(\mathbf{x})$ . Condition 2 (Task Alignment) implies  $p_{\text{SAE}}(y|\mathbf{x}) = p_{\text{true}}(y|\mathbf{x})$  almost everywhere. Combining these, the implicit conditional generative model of the SAE matches the true distribution:

$$p_{\text{SAE}}(\mathbf{x}|y) = p_{\text{true}}(\mathbf{x}|y) \quad (8)$$

Since  $\mathbf{x} = \mathbf{g}(\mathbf{z})$  is a diffeomorphism, we apply the change of variables formula:

$$p_{\text{true}}(\mathbf{x}|y) = p(\mathbf{z}|y) |\det J_{\mathbf{g}^{-1}}(\mathbf{x})| \quad (9)$$

Similarly for the learned representation  $\mathbf{a}$  (assuming implicit  $\mathbf{x} = \hat{\mathbf{g}}(\mathbf{a})$ ):

$$p_{\text{SAE}}(\mathbf{x}|y) = p_{\mathbf{a}}(\mathbf{a}|y) |\det J_{\mathbf{f}}(\mathbf{x})| \quad (10)$$

Taking the log-difference between two distinct responses  $y$  and  $y_0$ :

$$\log p(\mathbf{x}|y) - \log p(\mathbf{x}|y_0) = \log p(\mathbf{z}|y) - \log p(\mathbf{z}|y_0) \quad (11)$$

The Jacobian terms  $|\det J|$  depend only on  $\mathbf{x}$  (geometry of the mixing function) and cancel out in the subtraction, effectively isolating the contribution of the latent factors.

Substituting the exponential family form  $p(\mathbf{z}|y) \propto \exp(\mathbf{T}(\mathbf{z})^\top \boldsymbol{\lambda}(y))$ , the equation becomes:

$$\mathbf{T}(\mathbf{z})^\top (\boldsymbol{\lambda}(y) - \boldsymbol{\lambda}(y_0)) = \hat{\mathbf{T}}(\mathbf{a})^\top (\hat{\boldsymbol{\lambda}}(y) - \hat{\boldsymbol{\lambda}}(y_0)) + \text{const} \quad (12)$$

Given Condition 3 (Sufficient Variability), we can collect enough distinct responses  $y_1, \dots, y_k$  to form an invertible linear system. This implies that the learned sufficient statistics are an affine transformation of the true ones:

$$\mathbf{T}(\mathbf{z}) = \mathbf{A}\hat{\mathbf{T}}(\mathbf{a}) + \mathbf{b} \quad (13)$$

Assuming  $\mathbf{T}$  is linear (or component-wise invertible), this establishes an affine relationship  $\mathbf{z} \approx \mathbf{M}\mathbf{a}$ . The nonlinear mixing  $\mathbf{g}$  is thus resolved up to an affine transformation  $\mathbf{M}$ .

Finally, we invoke Condition 4 (Sparsity). We have a linear mixture  $\mathbf{a} = \mathbf{B}\mathbf{z}$ . Since the components of  $\mathbf{z}$  are independent and super-Gaussian (Laplacian), and the objective minimizes  $\mathbb{E}[\|\mathbf{a}\|_1]$ , Theorem 11 from (Comon, 1994) guarantees that the mixing matrix  $\mathbf{B}$  must be a generalized permutation matrix  $\mathbf{P}\boldsymbol{\Lambda}$  to achieve the minimum  $\ell_1$  norm. Therefore,  $\mathbf{a}$  recovers  $\mathbf{z}$  up to permutation and scaling.  $\square$

## C. Proof of Proposition 4.2

*Proof.* Based on Proposition 4.1, we have established that the SAE encoder  $\mathbf{f}$  identifies the true latent factors  $\mathbf{z}$  up to a linear transformation (specifically, a permutation and scaling). Thus, we can write the learned representation  $\mathbf{a}$  as:

$$\mathbf{a} = \mathbf{f}(\mathbf{x}) \approx \mathbf{P}\boldsymbol{\Lambda}\mathbf{z} + \mathbf{c} = \mathbf{P}\boldsymbol{\Lambda} \begin{bmatrix} \mathbf{s} \\ \mathbf{u} \end{bmatrix} + \mathbf{c}. \quad (14)$$

Since  $\mathbf{P}\boldsymbol{\Lambda}$  is a diagonal-like matrix (permuted diagonal), the components of  $\mathbf{a}$  are disjoint linear scalings of the components of  $\mathbf{s}$  and  $\mathbf{u}$ . We can decompose  $\mathbf{a}$  into  $\mathbf{a}_s$  (dimensions corresponding to  $\mathbf{s}$ ) and  $\mathbf{a}_u$  (dimensions corresponding to  $\mathbf{u}$ ).

Consider the difference vector  $\boldsymbol{\delta}$  between the representations of the paired inputs:

$$\boldsymbol{\delta} = \mathbf{f}(\mathbf{x}) - \mathbf{f}(\mathbf{x}^+) = (\mathbf{a}_s - \mathbf{a}_s^+) + (\mathbf{a}_u - \mathbf{a}_u^+). \quad (15)$$

Invoking the *Content Invariance* assumption,  $\mathbf{s} = \mathbf{s}^+$ , which implies  $\mathbf{a}_s = \mathbf{a}_s^+$ . Therefore, the task-related components cancel out:

$$\boldsymbol{\delta} = \mathbf{0} + (\mathbf{a}_u - \mathbf{a}_u^+). \quad (16)$$

Table 5. Examples of paired queries from our dataset. While all three inputs share the same malicious intent  $s$  (“make a bomb”), their surface representations  $u$  differ drastically:  $x_{\text{GCG}}$  relies on adversarial gibberish suffixes, while  $x_{\text{AutoDAN}}$  employs a semantic role-playing template. Our method identifies the invariant  $s$  despite these variations.

This demonstrates that the difference vector  $\delta$  lies entirely within the subspace spanned by the defense factors  $u$ . By applying orthogonalization (as defined in Equation 4), we project the representation  $a$  onto the subspace orthogonal to  $\delta$ . Let  $Q$  be the projection matrix. The filtered representation is:

$$\tilde{a} = Qa = Q(a_s + a_u). \quad (17)$$

Since  $\mathbf{a}_u$  lies in the direction of  $\delta$  (assuming for simplicity of proof that the variation covers the defense subspace),  $\mathbf{Q}\mathbf{a}_u \approx \mathbf{0}$ . The remaining term is  $\mathbf{Q}\mathbf{a}_s$ . Since  $\mathbf{a}_s$  is already an identifiable recovery of  $\mathbf{s}$  (from Prop 1), the filtered representation  $\tilde{\mathbf{a}}$  effectively isolates the task semantics  $\mathbf{s}$ , identifying it up to the remaining affine parameters (scaling and shift).  $\square$

## D. Details of Feature Selection via SAE and Contrastive Analysis

### D.1. Formal Definition of Paired Contrastive Dataset

This subsection formally defines the paired contrastive dataset used to capture the dynamic shifts in safety mechanisms. We define the **Base Harmful Set**  $\mathcal{D}_{\text{harm}} = \{x_{\text{harm}}^{(i)}\}_{i=1}^N$  as a collection of harmful queries from HarmBench that consistently trigger a “Refusal” response under normal conditions. Correspondingly, the **Successful Attack Set** is defined as  $\mathcal{D}_{\text{attack}} = \{x_{\text{attack}}^{(i,j)}\}_{j=1}^M$ , comprising samples generated by applying adversarial perturbations (via algorithms such as GCG, TAP, or PAIR) to the source queries. Crucially, this set includes only those adversarial variants that successfully induce a “Compliance” response. In the resulting paired tuples  $(x_{\text{harm}}, x_{\text{attack}})$ , the *core malicious intent* remains invariant, while task-irrelevant factors—specifically the context triggering defense mechanisms versus the bypass style—vary. An example is shown in Table 5

## D.2. Extraction of Sparse Feature Activations

This subsection details the extraction of sparse feature activations using SAEs and justifies the focus on the last token position. Let  $f_{l,k}(x)$  denote the activation value of the  $k$ -th latent variable in the  $l$ -th layer of the SAE given input  $x$ . Due to the causal masking mechanism of the Transformer architecture, the hidden state of the *last token* in the input sequence aggregates the comprehensive contextual semantics of the entire instruction (Geva et al., 2021; Meng et al., 2022). Consequently, we define the activation difference for the  $k$ -th feature at the last token position  $t_{\text{last}}$  as:

$$\Delta_{l,k}^{(i)} = \left| f_{l,t_{\text{last}},k}(x_{\text{harm}}^{(i)}) - f_{l,t_{\text{last}},k}(x_{\text{attack}}^{(i,j)}) \right| \quad (18)$$

To mitigate bias from instance-specific noise (e.g., artifacts from specific attack prompts) and ensure statistical robustness, we define the global **Differential Importance Score** as the average across all  $N$  pairs:

$$\delta_{l,k} = \frac{1}{N} \sum_{i=1}^N \Delta_{l,k}^{(i)} \quad (19)$$

### D.3. Feature Selection and Intent Isolation

This subsection elucidates how to isolate the purified intent  $S$  by filtering the defense feature  $S'_{\text{defense}}$  from high-difference candidates. First, we rank all latent features in the SAE dictionary in descending order based on  $\delta_{l,k}$  and retain the top- $K$  features to form the candidate set  $\hat{S}$ . However, this set may also contain template noise representations ( $S'_{\text{template}}$ ), which exhibit high variation in non-task contexts. Therefore, further refinement is required to accurately distinguish  $S'_{\text{defense}}$ . Based on the premise that task semantics are invariant, the core intent  $S$  should maintain globally low variance in activation difference. In contrast,  $S'_{\text{defense}}$  is characterized by **stable high activation (low variance)** within  $\mathcal{D}_{\text{harm}}$  (consistently triggering refusal) but exhibits drastic fluctuation (high variance) when shifting between datasets. We utilize this variance-based criterion to filter  $S'_{\text{defense}}$  from  $\hat{S}$ . Finally, we employ weight orthogonalization to physically strip the direction vector of  $S'_{\text{defense}}$  from the model parameters. We validate this isolation by observing if the removal induces a behavior flip from refusal to compliance on  $\mathcal{D}_{\text{harm}}$ . Upon successful validation, the remaining effective activation after excluding this confounding direction is formally defined as the front-door mediator  $S$ .

## E. Baselines

We benchmark CFAA against 5 baseline methods:

- **GCG** (Zou et al., 2023b): Token-level optimization of an adversarial suffix appended to the user prompt. This gradient-based method optimizes the suffix to maximize the log probability of the target LLM generating an affirmative response (e.g., "Sure, here is how").
- **PAIR** (Chao et al., 2024b): An iterative framework where an attacker LLM is prompted to adaptively generate and refine candidate prompts. It functions as a competitive game to explore the target model's vulnerabilities and elicit harmful behaviors.
- **TAP** (Mehrotra et al., 2024a): An enhancement of PAIR that utilizes tree-structured prompting (Tree of Thoughts). An attacker LLM explores the prompt space using a branching strategy to systematically find successful jailbreaks with fewer queries.
- **AutoDAN** (Liu et al., 2024a): A semi-automated method that combines handcrafted jailbreak templates with a hierarchical genetic algorithm. It evolves the prompt population to maintain stealthiness while optimizing for the elicitation of specific harmful behaviors.
- **PAP** (Zeng et al., 2024): A method focusing on persuasive strategies. It leverages an attacker LLM to rewrite the harmful request using various persuasion techniques (e.g., logical appeal, authority) to convince the target model to comply.
- **ICA** (Wei et al., 2023a): An In-Context Learning (ICL) based attack that exploits the model's pattern-following capability. By providing few-shot demonstrations of harmful query-response pairs, it induces a pattern of compliance that overrides the model's safety alignment.
- **ReNeLLM** (Ding et al., 2024): A framework based on prompt rewriting. It leverages a helper LLM to rephrase harmful queries into various benign-appearing scenarios (e.g., code completion, creative writing) to obscure malicious intent and evade input filters.
- **DeepInception** (Li et al., 2023): A method utilizing recursive context injection (often termed "hypnosis"). It constructs a multi-layered, nested fictional environment (e.g., a dream within a dream) to mislead the model into a state of personification, causing it to escape safety guardrails.

## F. LLMs

Our evaluation encompasses four representative open-source and safety-aligned LLMs.

- **Llama 3.1 8B Instruct** (Dubey et al., 2024): It features a significantly expanded context window and improved instruction-following capabilities compared to Llama 2, with updated safety alignment protocols.
- **Llama 2 7B Chat** (Touvron et al., 2023): This model was adversarially trained with multiple rounds of manual red teaming. It is widely considered a strong baseline defense, often exhibiting high robustness against gradient-based attacks.
- **Mistral 7B Instruct** (Jiang et al., 2023): We use the Instruct v0.2 version. While no specific safety measures were detailed in its training process, empirical observations show it possesses a baseline capability to refuse direct harmful requests.
- **Gemma2 9B Instruct** (Team et al., 2024): We utilize the instruction-tuned Gemma-2-9b-it, which is optimized via knowledge distillation and RLHF. Its alignment process incorporates rigorous safety reward modeling and data filtering, establishing robust refusal capabilities against harmful queries.

## G. Experimental Details

### G.1. Implementation Environment

All experiments were conducted on a high-performance computing cluster equipped with **5 × NVIDIA A100 (80GB GPUs)** to support the memory-intensive requirements of LLM inference and SAE activation caching. The implementation utilizes PyTorch 2.1 and the Transformers library 4.36. For the mechanistic interpretation pipeline, we leveraged the SAELens (Bloom et al., 2024) and TransformerLens (Nanda & Bloom, 2022) libraries, which provide optimized kernels for efficient sparse feature extraction.

### G.2. SAE Resources for Mechanistic Analysis

To ensure the reproducibility of our findings, we utilized state-of-the-art, open-source SAE checkpoints. We specifically selected lightweight configurations (lower expansion factors) to focus on the most fundamental and salient features. The details of the SAE resources for the four representative models are as follows:

- **Llama-3.1-8B-Instruct** (Dubey et al., 2024): We employed the checkpoints compatible with *SAE Lens*, focusing on the residual stream SAEs with a dictionary size of **32k** (Expansion Factor  $\approx 8$ ). This configuration effectively balances feature granularity and interpretability for safety-critical concepts (He et al., 2024a).
- **Gemma-2-9B-It** (Team et al., 2024): We utilized the official *Gemma Scope* release (Lieberum et al., 2024). We selected the **16k-width** SAEs (Expansion Factor  $\approx 4$ ) trained on the residual stream, which are optimized to capture core behavioral representations with minimal redundancy.
- **Mistral-7B-Instruct-v0.2** (Jiang et al., 2023): We adopted the community-standard SAEs from the *SAE-Lens* repository (Bloom et al., 2024), utilizing checkpoints with a dictionary size of **32k**. These are trained on 100M tokens of OpenWebText and provide robust coverage for instruction-following tasks.
- **Llama-2-7B-Chat** (Touvron et al., 2023): We leveraged the standard residual stream SAEs (width **32k**) available in the *SAE-Lens* library (Bloom et al., 2024). Using this consistent width allows for a fair comparative analysis of defense mechanisms across the Llama 2 and Llama 3 generations.

These pre-trained SAEs serve as the structural foundation for identifying the mediator  $S$ .

### G.3. Evaluation Protocols

In this work, we employ the official **HarmBench Classifier** (cais/HarmBench-Llama-2-13b-cls) (Mazeika et al., 2024) as the judge to evaluate the Attack Success Rate (ASR). Adopting this standardized evaluation protocol ensures

reproducibility and fair comparison with baselines. This classifier, fine-tuned on Llama-2-13b, is explicitly distilled to approximate GPT-4 based safety judgments, thereby providing a robust and consistent metric for distinguishing successful jailbreaks from refusals. The judge operates on a rigorous classification rubric